Yoshimori *et al. Progress in Earth and Planetary Science* (2016) 3:21
DOI 10.1186/s40645-016-0096-3

Progress in Earth and Planetary Science

REVIEW Open Access

A review of progress towards understanding the transient global mean surface temperature response to radiative perturbation

Masakazu Yoshimori[1,2*], Masahiro Watanabe[3], Hideo Shiogama[4], Akira Oka[3], Ayako Abe-Ouchi[3,5], Rumi Ohgaito[5] and Youichi Kamae[6]

Abstract

The correct understanding of the transient response to external radiative perturbation is important for the interpretation of observed climate change, the prediction of near-future climate change, and committed warming under climate stabilization scenarios, as well as the estimation of equilibrium climate sensitivity based on observation data. It has been known for some time that the radiative damping rate per unit of global mean surface temperature increase varies with time, and this inconstancy affects the transient response. Knowledge of the equilibrium response alone is insufficient, but understanding the transient response of the global mean surface temperature has made rapid progress. The recent progress accompanies the relatively new concept of the efficacies of ocean heat uptake and forcing. The ocean heat uptake efficacy associates the temperature response induced by ocean heat uptake with equilibrium temperature response, and the efficacy of forcing compares the temperature response caused by non-CO_2 forcing with that by CO_2 forcing.

In this review article, recent studies on these efficacies are discussed, starting from the classical global feedback framework and basis of the transient response. An attempt is made to structure different studies that emphasize different aspects of the transient response and to stress the relevance of those individual studies. The implications on the definition and computation of forcing and on the estimation of the equilibrium response in climate models are also discussed. Along with these discussions, examples are provided with MIROC climate model multi-millennial simulations.

Keywords: Transient climate response, Equilibrium climate sensitivity, Climate feedback, Ocean heat uptake efficacy, Efficacy of forcing

Introduction

A climate system is said to be in equilibrium when it exhibits a statistically stable state for an extended period of time under a given set of boundary conditions. When external radiative perturbation is added to the system (radiative forcing), it begins to reveal different statistical behavior, which includes the mean state. The statistical behavior evolves as time progresses, and the system eventually reaches a new equilibrium that is constrained by the newly imposed boundary conditions. Historically, the equilibrium response has received much attention; the equilibrium climate sensitivity (ECS) is the most notable example (Knutti and Hegerl 2008; Maslin and Austin 2012). The ECS is defined as the globally and annually averaged value of the equilibrium surface temperature response to a doubling of atmospheric CO_2 concentration. The ECS is an idealized yet useful concept, because it represents the final boundary of the system, and gives a measure of how much warming would occur in the future even if the current CO_2 concentration is sustained and not raised. We note that changes in

* Correspondence: myoshimo@ees.hokudai.ac.jp
[1]Faculty of Environmental Earth Science, Hokkaido University, Kita 10, Nishi 5, Kita-ku, Sapporo 060-0810, Japan
[2]Arctic Research Center, Hokkaido University, Sapporo, Japan
Full list of author information is available at the end of the article

vegetation and ice-sheet distributions and in atmospheric gas concentrations by a biogeochemical response are excluded from the formal definition of ECS, although the effect of vegetation change is sometimes included in recent model-based estimates. While ice sheets exhibit multiple equilibria (e.g., Abe-Ouchi et al. 2013), the ECS is an inherent property of the climate system, which is independent of the history of radiative forcing.

The transient response, which generally includes the effect of time-varying boundary conditions, is more complicated to characterize and understand than the equilibrium response. In addition, the system does not approach equilibrium at a constant rate even under constant radiative forcing. Nevertheless, the transient response has received more and more attention recently, because it is more relevant to near-future climate change and thus has more practical implications (Allen and Frame 2007). From the viewpoint of climate stabilization scenarios, understanding the transient response is also important for evaluating the magnitude of "committed" warming and the rate of the change accurately (Armour and Roe 2011; Meehl et al. 2005; Plattner et al. 2008; Solomon et al. 2009; Zickfeld et al. 2013). Here, the committed warming is referred to an additional surface warming that is expected to emerge when constant radiative forcing is continuously applied after a stabilization point.

In this review article, we focus on the transient response of the global mean surface temperature to external radiative perturbation, because the magnitudes of many climatic impacts can be scaled proportionally to this global mean variable relatively well (e.g., Ishizaki et al. 2012; Ishizaki et al. 2013; Yoshimori and Abe-Ouchi 2012). One of the motivations for this review arises from the recent, rapid conceptual development on climate feedbacks. Here, climate feedbacks are loosely defined as climate change processes that cause the additional radiative adjustment to the climate system in response to the initial radiative perturbation. For example, previously underappreciated factors such as spatiotemporally varying climate feedbacks related to the ocean heat uptake and the dependence of climate sensitivity on forcing agents have been identified as important. These factors are essential for a quantitative understanding of the transient response. Nevertheless, these factors are rather confusing and not necessarily understood widely by the climate science community. In addition, the recent progress requires further clarification of the definitions of forcing and feedback and discussions on how they are to be computed. It is becoming clear that the omission of such factors would introduce a bias into the estimate of ECS based on observation data. The understanding of the background long-term response to anthropogenic radiative perturbation must also be well established for clarifying observed contemporary climate variations, such as the warming pause or "hiatus" during the early twenty-first century (e.g., Kosaka and Xie 2013; Meehl et al. 2011; Watanabe et al. 2013; Watanabe et al. 2014).

Transient climate response in a global feedback framework

In this section, the transient response of the global mean surface temperature to radiative perturbation is reviewed in a classical global feedback framework. In this framework, the loss of radiative energy from the climate system, i.e., radiative damping, is formulated in proportion to the global mean surface temperature change. In the following, all variables represent global mean values unless noted explicitly. We start with an equilibrium state in which the global mean net radiation at the top of the atmosphere (TOA) is zero.

A classical definition of radiative forcing is instantaneous or stratosphere adjusted forcing in which the radiative perturbation is evaluated at the tropopause instantaneously (on the time scale of radiative transfer) after the perturbation is applied or after the stratospheric temperature responds radiatively to the perturbation. The tropopause is chosen because the troposphere and surface are tightly coupled thermally through radiation and convection. The adjustments of stratospheric temperature are included in the forcing because its response time is on the order of months, and the subsequent forcing thus represents a more effective measure of radiative effect on the troposphere-surface system (Hansen et al. 1997; Stuber et al. 2001). We note that the magnitude of radiative forcing at the TOA is the same as that at the tropopause after the stratospheric adjustments, because any vertical convergence of radiative fluxes in the stratosphere would cause local temperature to adjust (Hansen et al. 1997).

When radiative forcing F is applied to the TOA, the energy budget equation with the net TOA radiation, called N, may be written in the simplest form as

$$N = F - \lambda \Delta T \qquad (1)$$

where λ is termed the *climate feedback parameter* and represents how much energy is lost to space in accordance with the unit increase of the global mean surface temperature T (e.g., Gregory et al. 2015; Gregory et al. 2004; Knutti and Hegerl 2008; Winton et al. 2010). Symbol Δ denotes the deviation (or anomaly) from the unperturbed climate. Parameter λ must be positive in order for the system to eventually reach a stable state. We note that a "signed" feedback parameter, e.g., $\Lambda \equiv -\lambda$, which has a positive/negative value for the amplification/suppression of initial perturbation (i.e., positive/negative feedback), is also widely used in other literature (e.g., Armour et al. 2013; Boer and Yu 2003; Winton et al. 2013a). N reflects mostly ocean heat uptake with other forms of energy consumption being latent heat for snow/ice melting, for example (Rhein et al. 2013), and eventually diminishes to zero under constant radiative forcing.

When the feedback is distinguished from the forcing as the surface temperature-mediated response of the climate system as in Eq. (1), it is more consistent to include the so-called rapid tropospheric adjustments in the definition of forcing. The troposphere may respond to forcing directly and rapidly (typically, «1 year) without invoking a surface temperature change. Examples of the tropospheric adjustments include cloud response to lower tropospheric warming due to the increase in atmospheric CO_2 concentration (cloud adjustments, Gregory and Webb 2008), cloud albedo and lifetime changes due to the increase in aerosols (indirect effect of aerosols), and cloud amount changes due to the increase in light-absorbing aerosols (semi-direct effect of aerosols). The resulting forcing is referred to the stratosphere-troposphere-adjusted radiative forcing or *effective radiative forcing* (ERF). For details on the mechanism of tropospheric adjustments, readers are referred to Andrews et al. (2012a), Kamae et al. (2015), and Sherwood et al. (2015).

It is often assumed that λ is constant, i.e., $\lambda = \lambda_{eq}$ at equilibrium, which leads to the conclusion that the transient response (ΔT) to constant radiative forcing is always smaller than the equilibrium response (ΔT_{eq}). Therefore, a rewrite of Eq. (1) indeed gives

$$\Delta T = \frac{F-N}{\lambda} < \Delta T_{eq} = \frac{F}{\lambda_{eq}} \tag{2}$$

The time variation of λ is extensively discussed later. The global mean surface temperature change at the time of the doubled atmospheric CO_2 concentration (average of 61 to 80 years in practice) under a 1 % compound annual increase (1pctCO2 experiment of the Coupled Model Intercomparison Project 5 (CMIP5)) is termed *transient climate response* (TCR, Cubasch et al. 2001). The TCR satisfies

$$\mathrm{TCR} = \frac{F_{2\times}-N}{\lambda} < \mathrm{ECS} = \frac{F_{2\times}}{\lambda_{eq}} \tag{3}$$

where $F_{2\times}$ denotes the radiative forcing due to a doubling of the atmospheric CO_2 concentration. Figure 1 shows the TCR against ECS for the CMIP5 atmosphere-ocean general circulation models (AOGCMs) (Taylor et al. 2012), in which the TCR is indeed smaller than the ECS and a high correlation exists between the two (Flato et al. 2013).

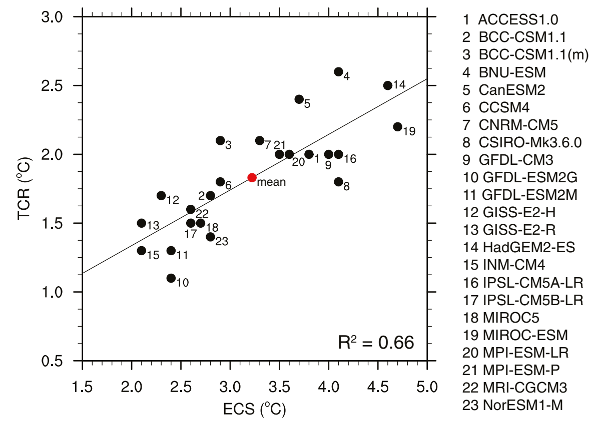

Fig. 1 Equilibrium climate sensitivity (ECS) and transient climate response (TCR) of 23 CMIP5 models. Redrawn from the data in Table 9.5 and Figure 9.42b in Flato et al. (2013). The linear regression line is also plotted. The *number at the lower right corner of the figure* indicates the fractional variance shared by ECS and TCR. The *right column* lists model names

Time scale of the response

In this section, the response time of the climate system is discussed, while still assuming that λ is constant. As stated above, N essentially reflects ocean heat uptake and may thus be expressed as

$$N = \frac{d(C\Delta T)}{dt} \tag{4}$$

where $C = \rho c_p h$ (ρ: density of seawater, c_p: specific heat of seawater at constant pressure, h: effective depth) is the effective heat capacity. Here, the term "effective" is used to represent the fact that the extent of penetration of the heat anomaly with respect to the unperturbed climate varies with time and space. A substitution of Eq. (4) with constant heat capacity into Eq. (1) yields

$$C\frac{d(\Delta T)}{dt} = F-\lambda\Delta T \tag{5}$$

At equilibrium, we obtain

$$\Delta T_{eq} \equiv \Delta T(t\to\infty) = \frac{F}{\lambda}, \tag{6}$$

and at the transient state, we obtain

$$\Delta T = \frac{F}{\lambda}\left(1-e^{-t/\tau}\right) \text{or} \frac{\Delta T}{\Delta T_{eq}} = 1-e^{-t/\tau} \tag{7}$$

where $\tau \equiv C/\lambda$ (Hansen et al. 1981; Hansen et al. 1984; Hansen et al. 1985; Wigley and Schlesinger 1985). Equation (7) means that ΔT reaches 63 % of ΔT_{eq} at $t = \tau$, and the rate depends on the effective heat capacity and the climate feedback parameter. Substitutions of $C = 2.1 \times 10^8$ or $C = 1.5 \times 10^{10}$ J K^{-1} m^{-2}, corresponding to a typical ocean mixed-layer depth (50 m) or the average depth of world oceans (3700 m), respectively, and a nominal value of $\lambda = 0.75$ W m^{-2} K^{-1} (corresponding to the ECS of about 3 °C), yield $\tau \cong 5$ or $\tau \cong 370$ years for the two ocean depths, respectively. The value of $\tau \cong 5$ does not include the effect of the heat exchange between the mixed layer and the deep ocean, and the $\tau \cong 370$ value assumes that the heat anomaly is communicated instantly throughout the water column. Both cases are unrealistic but give some insight into the response time. In reality, the heat anomaly spreads gradually from the surface to depth, and thus C varies with time. Schwartz (2007, 2008) applied a single-layer model with a similar formulation to estimate the ECS from the observation data, but their use of constant effective heat capacity for the entire climate system on all time scales of response was criticized (Foster et al. 2008; Knutti et al. 2008; Scafetta 2009). Donohoe et al. (2014) reported that the effective heat capacity is equivalent to about 50-m ocean depth during the first decade (consistent with our estimate of 5 years for the mixed-layer ocean) and equivalent to several hundred meters ocean depth after a century following an instantaneous quadrupling of atmospheric CO_2 concentration (abrupt4xCO2 experiment) for the CMIP5 AOGCMs.

As an intermediate model that ties the two limiting cases of box-ocean models with a mixed layer or with full depth, Gregory (2000) introduced the following two-layer ocean model to investigate the transient temperature response:

$$C\frac{d(\Delta T)}{dt} = F - \lambda\Delta T - H \text{ (upper ocean)} \tag{8}$$

$$C_D\frac{d(\Delta T_D)}{dt} = H \text{ (deep ocean)} \tag{9}$$

where the heat exchange between the two layers is assumed to be proportional to their difference in anomalous temperature with respect to the unperturbed climate:

$$H = \gamma(\Delta T - \Delta T_D) \tag{10}$$

where γ is the proportionality coefficient. The heat capacity of the atmosphere, land, and other surface components of the climate system is small and implicitly included in the heat capacity of the upper ocean (C), and C is much smaller than the heat capacity of the deep ocean (C_D), i.e., $C << C_D$. We note that the addition of Eqs. (8) and (9) yields Eq. (1). That is, the surface temperature change and the ocean heat uptake hold a linear relation under constant radiative forcing in the two-layer model. Geoffroy et al. (2013a) applied this model to analyze the CMIP5 AOGCM simulations and showed that the two-layer models tuned to emulate the global mean surface temperature response of AOGCMs in the abrupt4xCO2 experiment can also emulate the result of the slowly increasing CO_2 (1pctCO2) experiment reasonably well. This supports the assumption that the two-layer model is effective in capturing the minimal physics of the global mean surface temperature transient response.

The upper bound of the ocean response time can be estimated by the following scaling argument based on the fact that the important slow process of heat transport is vertical eddy diffusion:

$$\rho c_p\frac{d(\Delta T)}{dt} = \kappa_T\frac{\partial^2 T}{\partial z^2} \text{ or } \frac{d(\Delta T)}{dt} = \tilde{\kappa}_T\frac{\partial^2 T}{\partial z^2} \tag{11}$$

where κ_T is the *thermal conductivity* and $\tilde{\kappa}_T = \kappa_T/(\rho c_p)$ is the *thermal diffusivity* by eddies. A substitution of the effective value of $\tilde{\kappa}_T \sim 10^{-4}$ m^2 s^{-1} and $h = 3700$ m yields a time scale of about 4000 years ($\tau \sim h^2/\tilde{\kappa}_T$). Figure 2 shows the long-term integration of the MIROC3.2 AOGCM (K-1 model developers 2004) for the first 140 years of the 1pctCO2 experiment and the continuous integration under the four times constant CO_2 level (const4xCO2) experiment thereafter. For reference, the two times constant CO_2 level (const2xCO2) experiment, starting from 70 years of the 1pctCO2 experiment, is also plotted. We note that the equilibrium response of these experiments was studied in Yoshimori et al. (2014) and the entire simulations were used to study marine biogeochemical response in Yamamoto et al. (2014). While the surface air temperature responds to the forcing rather quickly, the ocean temperature changes much more slowly. The order of the time scale for the

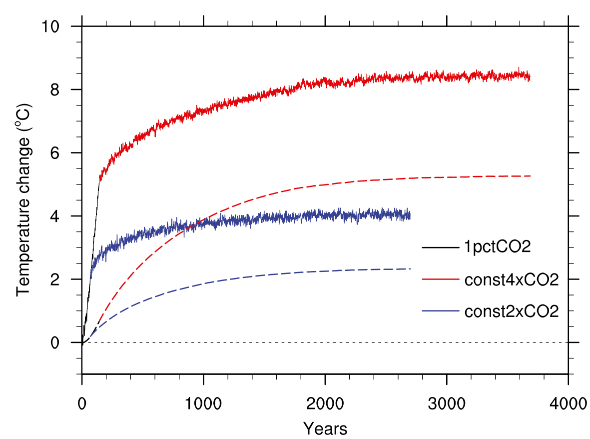

Fig. 2 Global and annual mean temperature changes from the preindustrial control simulation in the MIROC3.2 (medres) AOGCM experiments. *Solid lines*: surface air temperature; *dashed lines*: potential temperature averaged over the full ocean depth; *black lines*: 1 % compound annual increase of CO_2 (1pctCO2, 1–140 years); *blue lines*: constant 2xCO_2 forcing starting from year 70 of 1pctCO2 (const2xCO2, 71–2699 years); *red lines*: constant 4xCO_2 forcing starting from year 140 of 1pctCO2 (const4xCO2, 141–3685 years)

ocean to reach a new steady state in Fig. 2 is loosely consistent with the above estimate based on the scaling argument of 4000 years (i.e., 10^3 years). We note that multi-millennial simulations for the increased CO_2 concentration are not available for the CMIPs.

Traditionally, one-dimensional box-diffusion ocean models (Hansen et al. 1985; Long and Collins 2013; Siegenthaler and Oeschger 1984; Wigley and Schlesinger 1985) or upwelling-diffusion (UD) ocean models (Andronova and Schlesinger 2001; Baker and Roe 2009; Johansson et al. 2015; Wigley and Raper 2001) have been used. AOGCM studies, however, point out the following limitations of such models: (a) the deep convection at high latitudes identified as an important process in AOGCMs is not properly represented (Gregory 2000); (b) the vertical structure of the heat anomaly stored in the UD ocean models is biased to a shallower depth as compared to an AOGCM (Li et al. 2013); and (c) the total heat anomaly stored in the UD ocean models, which corresponds to the thermosteric sea level rise, is underestimated as compared to an AOGCM (Li et al. 2013).

Kostov et al. (2014) showed that the time scale of the penetration depth of the heat anomaly with respect to the unperturbed climate is positively correlated with the depth and strength of the Atlantic meridional overturning circulation (AMOC) on a century time scale in the eight CMIP5 AOGCMs. This result suggests that the AMOC plays an important role in setting the rate of global ocean heat uptake. In addition to the AMOC, Marshall and Zanna (2014) used a conceptual model to point out the importance of ocean eddy mixing in the Southern Ocean, with larger mixing leading to a faster (yet smaller) global heat uptake response.

Ocean heat uptake efficiency

The ocean heat uptake under the monotonically increasing radiative forcing is often approximated by

$$N = \kappa \Delta T \tag{12}$$

where κ is called the *ocean heat uptake efficiency* (Gregory and Mitchell 1997; Raper et al. 2002). It is assumed that κ is either constant or slowly varies with ΔT. Physically, Eq. (12) represents that heat exchange between the upper and deep oceans occurs in proportion to the surface temperature change and that the deep ocean is implicitly assumed to have an infinite heat capacity with a constant temperature. This assumption imposes a major limitation on the use of ocean heat uptake efficiency; however, it should be noted that this limitation does not affect the two-layer ocean model introduced earlier. Indeed, Eq. (12) can be derived from Eqs. (8)–(10) by assuming that the total ocean heat uptake is dominated by the deep ocean ($N \approx H$) and by replacing γ with κ. Equation (12) is invalid for a transient response immediately after a rapid change in radiative forcing ($N \approx F, \Delta T \approx 0$; e.g., abrupt4xCO2 experiment) as it requires an infinite κ. Equation (12) is also invalid on long time scales and in particular near equilibrium because κ approaches zero when the transient response becomes close to the equilibrium ($N \approx 0, \Delta T \neq 0$). Figure 3 shows a schematic diagram of the relation between ΔT and N after a step increase in radiative forcing, where κ represents the slope of the line (thin black line) pointing from the origin to a state in the simulation (a point in the thick black curve). An example of a monotonically increasing CO_2 (1pctCO2) experiment is presented by the black crosses in Fig. 4. Approximate linearity is observed except for the initial warming period, thereby supporting the general validity of Eq. (12) in this case.

The CMIP5 AOGCM simulations of recent climate change showed that κ decreases with time (Watanabe et al. 2013). This result could reflect less heat uptake in more stratified ocean, i.e., faster warming in the upper ocean that suppresses vertical mixing, or warming of the deep ocean that weakens the effect of mixing. Figure 5a displays the relation between the surface air temperature change and the temperature changes for four oceanic layers of different depths. The figure shows that the upper 300 m of ocean warms at half the speed of the surface air and the ocean below 1000 m warms slightly.

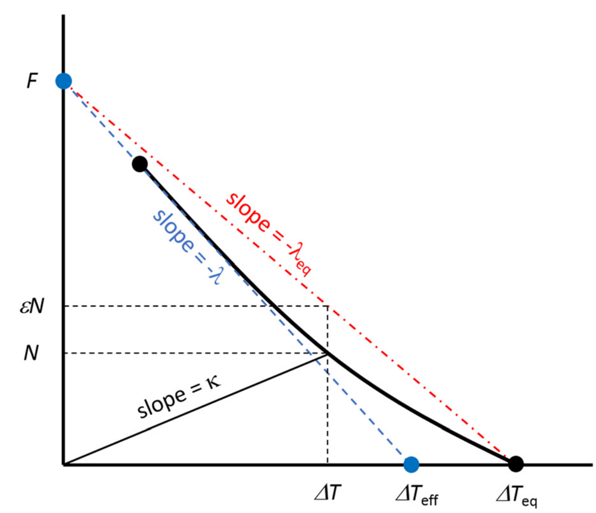

Fig. 3 Schematic diagram of the summary of concepts developed for understanding of the transient response of the global mean surface temperature. The *horizontal* and *vertical axes* are surface temperature and TOA net radiation changes after a step increase in radiative forcing, respectively. Figure A1 of Winton et al. (2013a) is referenced. *N*: TOA net radiation change; *F*: effective radiative forcing; ΔT: transient temperature change; λ: (effective) climate feedback parameter; λ_{eq}: equilibrium climate feedback parameter; κ: ocean heat uptake efficiency; ε: ocean heat uptake efficacy; ΔT_{eff}: effective climate sensitivity (in the case of $2xCO_2$ forcing); ΔT_{eq}: equilibrium temperature change. See the text for the details

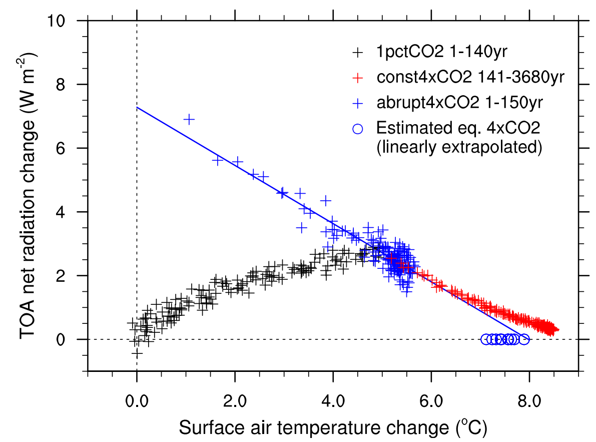

Fig. 4 Relation between global mean surface air temperature and TOA net radiation changes from the preindustrial control simulation in the MIROC3.2 (medres) AOGCM experiments. *Black crosses*: 1pctCO2 experiment (every year for 1–140 years); *blue crosses*: abrutp4xCO2 experiment (every year for 1–150 years); *red crosses*: const4xCO2 experiment (every 20-year average for 141–3680 years); *blue line*: linear regression for the 150-year abrupt4xCO2 experiment; *blue circles*: equilibrium temperature response to $4xCO_2$ estimated by Gregory's method for 10 abrupt4xCO2 20-year-long ensemble experiments (that start from different initial conditions in the preindustrial control simulation)

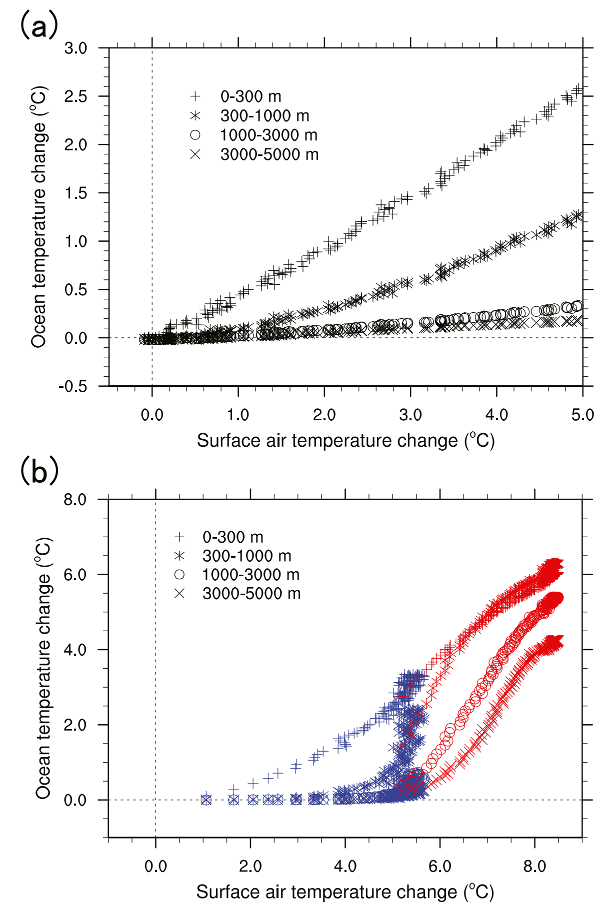

Fig. 5 Global mean ocean temperature changes at four different depth layers from the preindustrial control simulation in the MIROC3.2 (medres) AOGCM experiments. The changes are plotted as functions of the surface air temperature change. **a** 1pctCO2 experiment (every year for 1–140 years). **b** abrupt4xCO2 experiment (*blue*, every year for 1–150 years) and const4xCO2 experiment (*red*: every 20-year average for 141–3680 years)

Thus, Fig. 5a indicates that the vertical stratification is reduced on a centennial scale. Similarly, Fig. 5b displays the millennial scale of the ocean temperature change with respect to the surface air temperature change. The figure shows that the ocean temperature below 1000 m reaches the upper ocean warming after about a century, although temperature changes never reach the same magnitude. This result suggests that the effect of vertical mixing might become smaller. It also shows that the upper ocean does not warm as much as the surface air at the equilibrium.

The ocean heat uptake efficiency is contrasted with the climate feedback parameter. The substitution of Eq. (12) into Eq. (1) yields

$$F = \rho \Delta T \tag{13}$$

where $\rho \equiv \kappa + \lambda$ is termed the *climate resistance* (Gregory and Forster 2008; Gregory et al. 2009, 2010). Here, κ reflects primarily oceanic processes and a larger value indicates that more of the heat anomaly is absorbed in the ocean and hence surface warming is suppressed. On the other hand, λ reflects primarily the atmospheric processes (and sea ice-albedo feedback) and the larger value indicates that excessive energy is more effectively lost to space. The resistance ρ depends on κ (oceanic process) and λ (atmospheric process), and as a result of both processes, the surface temperature change remains small when resistance ρ is large.

By assuming $\lambda = \lambda_{eq}$, arranging Eq. (2) and Eq. (12) yields

$$\frac{\Delta T}{\Delta T_{eq}} = \frac{1}{1 + \kappa/\lambda} \tag{14}$$

As indicated by Eq. (14), the ratio of transient warming to equilibrium warming is larger when κ is smaller or λ is larger. We note that a case of large λ is consistent with Eq. (7). Raper et al. (2002) found a negative correlation between κ and λ in nine CMIP2 AOGCMs. They noted that larger surface warming caused by the smaller radiative damping rate of λ accompanies stronger ocean stratification and less heat release from the interior of the ocean through convection at high latitudes. This relation corresponds to a larger net heat uptake of the global ocean, i.e., a larger κ In the unperturbed climate, the AMOC transports heat to the northern high latitudes, where heat is released to the atmosphere. The AMOC acting as a heat sink of the ocean was reported by Knutti and Stocker (2000) and Marshall and Zanna (2014). The negative correlation found by Raper et al. (2002) was not verified in later studies with a larger number of models, however (Geoffroy et al. 2013a; Gregory and Forster 2008; Plattner et al. 2008). We note that Kuhlbrodt and Gregory (2012) emphasized the dominant role of the Southern Ocean and found the importance of eddy-induced transport in the model discrepancies of global ocean heat uptake.

Dufresne and Bony (2008) used Eq. (12) to quantify the relative contribution of radiative forcing, ocean heat uptake, and climate feedbacks to the spread of the TCR as well as the ECS in the CMIP3 AOGCMs. They concluded that cloud feedback is the predominant factor for the spread of both quantities. Boe et al. (2010), on the other hand, found a positive correlation in the CMIP3 AOGCMs between present-day ocean mixed-layer depths and future deep ocean warming and concluded that ocean heat uptake plays a major role in the uncertainty of transient warming, given that deep ocean warming is negatively correlated with surface temperature. Their analysis was based on the correlation of a single factor and so does not compare quantitatively with other factors, such as radiative forcing and climate feedbacks.

Effective climate sensitivity and ocean heat uptake efficacy

To discriminate the temperature change estimated by using the feedback parameter during the transient period from the ECS, the term *effective climate sensitivity* was introduced (Murphy 1995; Senior and Mitchell 2000) and is defined as follows:

$$\Delta T_{\mathrm{eff}} \equiv \frac{F_{2\times}}{\lambda} = \frac{F_{2\times}\Delta T}{F - N} \tag{15}$$

While Watterson (2000) showed that ΔT_{eff} is stable over time, numerous studies reported that ΔT_{eff} varies with time or is different from the ECS (e.g., Armour et al. 2013; Bitz et al. 2012; Boer and Yu 2003; Gregory et al. 2004; Kiehl et al. 2006; Li et al. 2013; Long and Collins 2013; Murphy 1995; Senior and Mitchell 2000; Williams et al. 2008; Winton et al. 2010).

In applying Eq. (15), stratosphere adjusted radiative forcing or ERF was used for F. One way to estimate the ERF is the regression method by Gregory et al. (2004), in which the ERF is given by the intercept at $\Delta T = 0$ of the ΔT-N linear regression after a step increase of forcing, if assuming Eq. (1). The blue colors in Fig. 4 represent the result of the abrupt4xCO2 experiment, and the blue crosses represent the global and annual mean anomalies for the initial 150 years. The regression line by Gregory's method is indicated by a blue line, which gives an ERF of 7.3 W m^{-2} at the y-intercept. In Fig. 3, the regression line by Gregory's method is indicated by a blue dashed line, and the ERF and effective climate sensitivity are denoted by F and ΔT_{eff}, respectively.

Williams et al. (2008) proposed *effective forcing*, in which the feedback parameter remains constant in time. Their effective forcing is different from the ERF by Gregory's method in that Williams applied linear regression for the stabilization period under constant forcing after 70 years of a monotonic CO_2 increase (1pctCO2) experiment and thus included an initial adjustment of the climate system on the decade level. Winton et al. (2010) argued that the decadal scale adjustment clearly contains the oceanic changes, and hence, it is more appropriate to regard the adjustment as a part of the feedback, rather than as a part of the forcing. Winton introduced a new parameter termed *ocean heat uptake efficacy* (ε), which is described in detail below.

In general, the TOA radiative anomaly induced by a unit surface temperature change during the transient period (λ) is different from that at equilibrium (λ_{eq}). This led Winton et al. (2010) to decompose the temperature response into equilibrium (ΔT_{eq}) and disequilibrium (or remaining) components, such that $\Delta T' \equiv \Delta T_{\mathrm{eq}} - \Delta T$

$$\Delta T_{\mathrm{eq}} = F/\lambda_{\mathrm{eq}} \tag{16}$$

$$\Delta T' = \varepsilon N/\lambda_{\mathrm{eq}} \tag{17}$$

without using the time-variant λ. Combining Eqs. (16) and (17) yields

$$\varepsilon N = F - \lambda_{\mathrm{eq}}\Delta T \tag{18}$$

Therefore, ΔT for a given ocean heat uptake N under a known forcing is determined by a single time-varying parameter ε. We note that Eqs. (16)–(18) correspond to the red dash-dot line in Fig. 3. The feedback parameter is introduced for the ocean heat uptake, λ_{o}, such that

$$N \equiv \lambda_{\mathrm{o}}\Delta T', \tag{19}$$

and substitution into Eq. (17) (Rose et al. 2014) yields

$$\varepsilon = \lambda_{\mathrm{eq}}/\lambda_{\mathrm{o}} \tag{20}$$

Here, Eq. (20) means that the ocean heat uptake efficacy parameter represents the ratio between feedbacks operating under radiative forcing and ocean heat uptake alone.

The ocean heat uptake efficacy is analogous to the *efficacy of forcing*. The efficacy of forcing is defined as the ratio of ΔT caused by a specific forcing agent to that induced by the CO_2 of the equivalent radiative forcing

(Hansen et al. 1997; Hansen et al. 2005; Yoshimori and Broccoli 2008):

$$\varepsilon_f \equiv \frac{\Delta T_{\text{non-CO}_2}/F_{\text{non-CO}_2}}{\Delta T_{\text{CO}_2}/F_{\text{CO}_2}} = \frac{\lambda_{\text{CO}_2}}{\lambda_{\text{non-CO}_2}} \tag{21}$$

In other words, the efficacy parameter of forcing represents the ratio between feedbacks operating under CO_2 and non-CO_2 forcing alone. To emphasize the similarity to Eqs. (16) and (17), Eq. (21) is written as

$$\Delta T_{\text{CO}_2} = F_{\text{CO}_2}/\lambda_{\text{CO}_2}, \tag{22}$$

$$\Delta T_{\text{non-CO}_2} = \varepsilon_f F_{\text{non-CO}_2}/\lambda_{\text{CO}_2} \tag{23}$$

Combining Eqs. (16) and (17), we obtain

$$\frac{\Delta T}{\Delta T_{\text{eq}}} = 1 - \frac{\varepsilon N}{F} \tag{24}$$

As long as Eq. (12) is valid, Eq. (24) is also expressed as

$$\frac{\Delta \text{T}}{\Delta T_{\text{eq}}} = \left(1 + \frac{\varepsilon \kappa}{\lambda_{\text{eq}}}\right)^{-1} \tag{25}$$

Therefore, Eq. (25) indicates that larger ocean heat uptake efficacy or efficiency leads to a smaller ratio of transient warming to equilibrium warming (Winton et al. 2010).

Geoffroy et al. (2013a) extended the study of Geoffroy et al. (2013b) by applying the following modified version of the two-layer model proposed by Held et al. (2010):

$$C\frac{d(\Delta T)}{dt} = F - \lambda_{\text{eq}}\Delta T - \varepsilon_0 H \text{ (upper ocean)} \tag{26}$$

$$C_D\frac{d(\Delta T_D)}{dt} = H \text{ (deep ocean)} \tag{27}$$

where ε_0 is a constant parameter of ocean heat uptake efficacy. By rewriting, Eq. (26) is more easily compared with Eq. (8)

$$C\frac{d(\Delta T)}{dt} = F - \lambda_{\text{eq}}\Delta T - H + (1 - \varepsilon_0)H \tag{28}$$

The last term on the right side represents the time-varying effect of λ, as explained below.

By combining Eqs. (26) and (27), the ocean heat uptake is written as

$$\begin{aligned} N &= C\frac{d(\Delta T)}{dt} + C_D\frac{d(\Delta T_D)}{dt} \\ &= F - \lambda_{\text{eq}}\Delta T - (\varepsilon_0 - 1)H \end{aligned} \tag{29}$$

In Fig. 3, Eq. (29) ties the two limiting cases for the slope α of the ΔT-N relation: Eq. (29) represents $\alpha = -\lambda_{\text{eq}} - \varepsilon_0\gamma$ while the surface temperature is initially adjusting to the imposed forcing ($\Delta T_D << \Delta T$) and the upper ocean dominates the total ocean heat uptake. Then, $\alpha = -\lambda_{\text{eq}}/\varepsilon_0$ while the deep ocean temperature is catching up with the surface warming ($\Delta T_D \propto \Delta T$) and the deep ocean dominates the total ocean heat uptake. Again, the efficacy parameter (ε_0) is assumed to be constant. We note the similarity of Eq. (29) to Eq. (18) in Eq. (30):

$$N = F - \lambda_{\text{eq}}\Delta T - (\varepsilon - 1)N \tag{30}$$

However, Eqs. (29) and (30) are equivalent ($N = H$) only when the heat uptake by the upper ocean Eq. (26) is much smaller than that by the deep ocean Eq. (27). We also note that no piecewise behavior is assumed in Eq. (18); the time-varying efficacy parameter (ε) captures the curvature of the slope in Fig. 3. According to Geoffroy et al. (2013a), the model with ocean heat uptake efficacy mimics the CMIP5 AOGCM simulations more closely because it can represent nonlinearity between the surface temperature change and the ocean heat uptake under constant radiative forcing. An example of the nonlinear curvature of the ΔT-N relation in an AOGCM is denoted by the blue and red crosses in Fig. 4. The equilibrium temperature response estimated by Gregory's method using the initial 20-year (blue circles) or 150-year integration (blue line) in the abrupt4xCO2 experiment tends to be smaller than the "true" equilibrium temperature response obtained from the long millennial integration.

Geoffroy et al. (2012) demonstrated that the spread of the TCR in the CMIP5 AOGCMs is caused by climate feedbacks (λ_{eq}), radiative forcing (F), and ocean heat uptake efficacy (ε_0), in the order of large to small contributions. Their result is consistent with that of Dufresne and Bony (2008) and leads to the conclusion that the uncertainty in cloud feedback is a dominant factor to the uncertainty in both ECS and TCR.

Time dependence of global feedbacks and physical meaning of ocean heat uptake efficacy

Armour et al. (2013) emphasized the advantage of a local/regional feedback framework, in which feedbacks are formulated as the TOA radiative anomaly per unit local surface temperature change, rather than per unit global mean surface temperature change (i.e., global feedback framework). In their local feedback framework, radiative damping is approximated by

$$\lambda(t)\Delta T(t) = \overline{\lambda(r,t)\Delta T(r,t)} \approx \overline{\lambda(r)\Delta T(r,t)}, \tag{31}$$

where r denotes location and the overbar represents the global average of local variables. The time variation of global mean radiative damping is therefore determined by the time-invariant local feedback parameter $\lambda(r)$ and the time-varying spatial pattern of surface temperature change $\Delta T(r,t)$. If there is no change in the horizontal energy transport of the atmosphere to compensate, the local ocean heat uptake and the corresponding net TOA radiation must be balanced by the local radiative damping to reach equilibrium. Thus, the shift of ocean heat uptake to the region of a less positive local feedback parameter means greater surface warming remains to occur before the equilibrium. In this local feedback framework, an increase of ocean heat uptake efficacy is interpreted as the region of ocean heat uptake shifting to the region of the less positive local feedback parameter, such as that for subpolar oceans. Figure 6 shows the anomalous sea surface temperature (SST) patterns at different times of the increasing CO_2 experiment in (a) and (b) and their difference in (c). The surface warming is more dominant in high latitudes at later times presumably because of the large effective heat capacity in the Southern Ocean and the progress in the Arctic sea ice melting. The difference in the local feedback parameters between low and high latitudes is the time-dependent global mean radiative feedback parameter. As an extension, a larger efficacy of forcing is interpreted as the radiative forcing applied to the region having the less positive local feedback parameter. In an idealized model configuration, Rose et al. (2014), however, showed that local feedback parameters can be sensitive to the latitudinal difference in ocean heat uptake. Because the pattern of ocean heat uptake varies with time, their result challenges the validity of the assumption that local feedback parameters are fixed in time. By conducting atmospheric general circulation model (AGCM) experiments with a fixed SST pattern (scaled by the global mean surface temperature change), Andrews et al. (2015) verified that the time variation of the global feedback parameter develops from the evolving pattern of surface temperature change. They also questioned whether that the local feedback framework explains everything. The dynamical effect of the atmosphere on local feedback parameters, therefore, requires further study (Feldl and Roe 2013; Rose et al. 2014).

Winton et al. (2013b) proposed an indirect radiative influence of the AMOC. They argued that weakening of the AMOC under global warming reduces the heat transport to the northern high latitudes and that corresponds to a shift of ocean heat uptake regions from low to high latitudes. This shift results in the increase of the ocean heat uptake efficacy and slows down the global surface temperature rise. As mentioned already, Kostov et al. (2014), on the other hand, proposed that the stronger AMOC enhances the penetration of the heat anomaly into deeper ocean in the perturbed climate, and the resulting increase in the effective heat capacity of the climate system slows down the global surface temperature rise. Therefore, the quantitative contribution of the AMOC still needs to be established.

Meraner et al. (2013) argued another aspect of inconstancy of the global feedback parameter, in which the

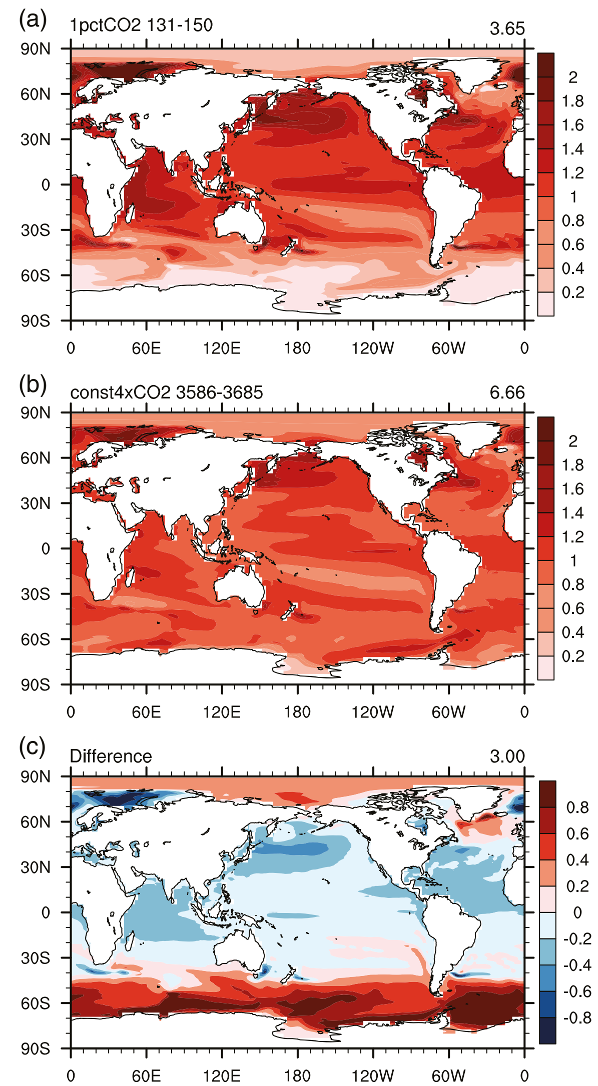

Fig. 6 SST changes normalized by the global mean SST changes from the control: **a** at the time of quadrupled CO_2 concentration in the 1pctCO2 experiment (average of 131–150 years); **b** at equilibrium in the const4xCO2 experiment (average of 3586–3685 years); and **c** the difference between **b** and **a**. The *number at the upper right corner of each figure* indicates the global mean SST changes from the control in degree Celsius

parameter becomes less positive and hence the ECS becomes larger in a warmer climate through enhanced water vapor feedback. The state dependency of climate feedbacks has been discussed in many previous studies (e.g., Colman and McAvaney 2009; Colman et al. 1997; Feldl and Roe 2013; Hansen et al. 2005; Jonko et al. 2013; Yoshimori et al. 2011), but the result appears to depend on the model and so the effect of the dependency on the transient response still needs to be established. In a similar context, the possibility of inconstancy of the climate resistance parameter (as well as the global feedback parameter) in the CMIP5 AOGCMs was reported by

Gregory et al. (2015), although they also listed errors in the estimated radiative forcing as an alternate or additional possibility.

In summary, time-varying global feedbacks or radiative damping may arise from (a) the state dependency of climate feedbacks, that is, the global feedback parameter depends on the background temperature T; (b) changes in the spatial pattern of the surface temperature anomaly $\Delta T(r,t)$ associated with ocean heat uptake and dynamics (ocean heat uptake efficacy) or forcing agent (efficacy of forcing); and (c) the non-local effect of atmospheric dynamics resulting from (b) on the local feedback parameter $\lambda(r,t)$.

Definitions and estimates of forcing

The time variation of the global climate feedback parameter has implications for how forcing and feedback are to be defined and computed. As discussed already, the nonlinearity of the relation between surface temperature and net radiation changes may introduce an error or arbitrariness into the estimate by Gregory's method. By using Eq. (1), a more general time-varying radiative forcing was estimated by Forster et al. (2013), but the global climate feedback parameter was necessarily assumed to be independent of the forcing agent and also time invariant. In addition to Gregory's method, the ERF was computed by using the fixed SST method by Hansen et al. (1997) and Hansen et al. (2005). In Hansen's method, the AGCM was run to equilibrium under constant forcing without allowing the SST to change. Because the typical time scale of adjustments was shorter than a year, Hansen's method might be applicable to time-varying forcing as well. The notable difference between Gregory's and Hansen's methods is that only the global surface temperature change is constrained to zero in Gregory's method. On the other hand, a local SST change is not allowed in Hansen's method, although it allows the land surface temperature to respond (Shine et al. (2003) suppressed the land surface response as well as SST change). A high correlation exists between the two methods, but Gregory's method tends to estimate a smaller ERF than does Hansen's method (Fig. 7). In both cases, the precise time scale of the adjustments is somewhat ambiguous. While the regression method is useful to investigate the relative spread among models (Andrews et al. 2015; Andrews et al. 2012b), it is expected that magnitude of forcing depends on the choice of period during the transient response, because the ΔT-N relation is nonlinear in general (Andrews et al. 2012b; Chen et al. 2014; Gregory et al. 2004; Winton et al. 2010). We note that the dominant factor of the model spread of the CO_2 ERF is still instantaneous forcing, not tropospheric adjustments (Chung and Soden 2015). As mentioned already, the effective forcing introduced by Williams et al. (2008) precludes the definition of feedback as a surface temperature-mediated response, because the decadal adjustments include the SST change.

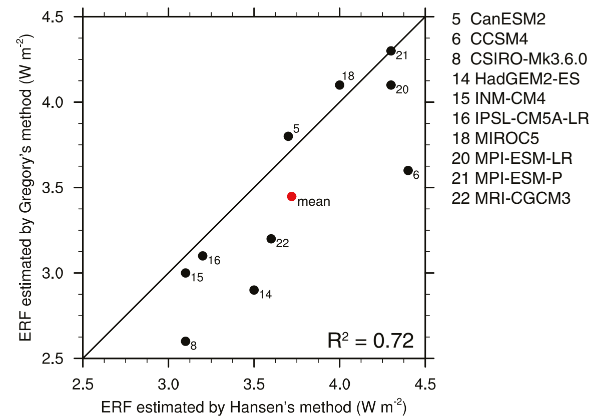

Fig. 7 Effective radiative forcing for the doubling of atmospheric CO_2 concentration estimated with Hansen's method and Gregory's method for 10 CMIP5 models. See the text for the details. The data taken from Table 9.5 of Flato et al. (2013). The one-to-one line is also plotted. The *number at the lower right corner of the figure* indicates the fractional variance shared by the two variables. The *right column* lists the model names with their numbers, which are identical to those in Fig. 1

Implication for the estimate of ECS

As stated in an earlier section, it takes a couple of millennia for a comprehensive climate model or AOGCM to reach a new equilibrium. Therefore, AOGCMs are not routinely run to equilibrium, and the ECS is not obtained precisely by following the definition. Traditionally, atmospheric GCMs coupled to "slab" mixed-layer ocean models (ASGCMs) are used to obtain the ECS. The mixed layer usually has a small yet sufficiently large heat capacity to simulate the annual cycle, and the steady state without considering the change in ocean dynamics is obtained after a few decades of integration. While some ASGCMs exhibit reasonably close ECSs to those obtained by the long integration of AOGCMs, other studies point out the difference (Danabasoglu and Gent 2009; Li et al. 2013; Shell 2013; Stouffer and Manabe 1999; Yokohata et al. 2008). Gregory's method was adapted by Andrews et al. (2012b) for the CMIP5 AOGCM analysis. It is expected that the linear part of the ΔT-N relation at the later stage of integration (fitting a line to the simulated trajectory closer to the equilibrium point in Figs. 3 and 4) yields an accurate ECS (Armour et al. 2013). Geoffroy et al. (2013a) applied the two-layer energy balance model with the ocean heat uptake efficacy parameter to the CMIP5 AOGCMs and estimated the optimal ECS and other parameters simultaneously. As a consequence, the model captures the nonlinearity of the ΔT-N relations. Although the mean of 16 estimated ECSs differs by only about 8 % compared to that estimated by the ocean heat uptake efficacy parameter of one (Geoffroy et al. 2013b), the difference is more than 20 % for the two AOGCM cases.

The nonlinearity occurring from the time variation of the global climate feedback parameter or the ocean heat uptake efficacy has a very important implication when the ECS is estimated from observation data. A general tendency of the global climate feedback parameter that is decreasing or the ocean heat uptake efficacy that is larger than one indicates that the ECS based on the energy budget may be underestimated when the transient data are used (Geoffroy et al. 2013a; Winton et al. 2010). In other words, the deviation of the effective climate sensitivity from the equilibrium climate sensitivity illustrated in Fig. 3 is not negligible, as pointed out in many studies (e.g., Armour et al. 2013; Rose et al. 2014; Winton et al. 2010). Because the observed data represent the transient stage of the response under increasing greenhouse gas forcing, this deviation is a concern for the observation-based estimate of the ECS (e.g., Forster and Gregory 2006; Gregory et al. 2002; Lewis and Curry 2015; Otto et al. 2013). The inconstancy of the climate resistance parameter yields similar concerns if the ECS estimate is made based on the assumption of its constancy (Gregory et al. 2015; Gregory and Forster 2008). We note that the efficacy of forcing is another important factor that may distort the estimate of the ECS from observations, as pointed out by Kummer and Dessler (2014), Shindell (2014), and Shindell et al. (2015). Marvel et al. (2015) argued that the best estimate of the TCR moves upward from 1.3 to 1.8 °C and the ECS from 2.0 to 2.9–3.0 °C if the efficacy of forcing based on a single model is taken into account. Therefore, even though the time variation of the climate feedback parameter is taken into account, the lack of the forcing efficacy factor (e.g., Masters 2014) may introduce bias in the ECS estimate. So far, the time variation of the forcing efficacy has not been well established. While climate models of reduced complexity enable us to constrain the ECS and TCR with statistical inference by conducting a large ensemble of parameter perturbations, we must not overlook the fact that the effect of the ocean heat uptake efficacy and the forcing efficacy are usually not taken into account (e.g., Aldrin et al. 2012; Skeie et al. 2014). This is not only limited to the ECS estimate based on historical observations but also is closely related to the ECS estimate based on a volcanic event (Merlis et al. 2014) or a past climate (Yoshimori et al. 2009).

Conclusions

Correct understanding of the transient response to radiative perturbation is important for the interpretation of observed climate change, the prediction of near-future climate change, and committed warming under climate stabilization scenarios, as well as the estimation of ECS based on observation data. It has been known for some time that the radiative damping rate per unit of global mean surface temperature increase (i.e., global climate feedback parameter) varies with time. This inconstancy affects the transient global mean surface temperature change, and different studies have emphasized the various different aspects of this inconstancy.

Recent progress has focused not only on the speed of the ocean heat uptake but also the spatial pattern of the ocean heat uptake. The spatial pattern influences the global radiative damping and thus the global climate feedback parameter. These influences arise from the evolving spatial pattern of the surface temperature anomaly and/or changes in the local feedback parameter. The inconstancy of the global climate feedback may be formulated by a single parameter, called ocean heat uptake efficacy. In addition, the dependency of the global climate feedback parameter on the background climate has also been pointed out. The physical mechanisms behind the behavior of the global climate feedback parameter still need to be established. Detailed analysis of the atmosphere-ocean interaction as well as perturbed physics ensemble experiments including the ocean component might be useful for identifying the physical mechanisms (Collins et al. 2006). Ocean heat uptake processes associated with the AMOC and those operating in the Southern Ocean are of great importance in understanding both speed and spatial pattern of ocean heat uptake and require further study.

The efficacy of forcing is another important factor determining the transient response to radiative perturbation. The current understanding of the forcing efficacy is very limited, and its time variation is particularly not well understood. Nevertheless, its inconstancy is presumed to be in the latitudinal distribution of forcing that varies with time.

All of these studies require the estimate of radiative forcing in a consistent manner. As proposed by Radiative Forcing Model Intercomparison Project,[1] ERF estimated by using AGCMs with a fixed SST, which does not require extrapolation, would greatly advance the study in a more quantitative way. Because the extrapolation using the regression technique in estimating the ECS would introduce ambiguity, we emphasize the usefulness of the integration of AOGCMs to equilibrium under doubled and quadrupled CO_2 forcing as presented in this review article and other studies with different ocean parameterizations (Yamamoto et al. 2015; Yamamoto et al. 2014).

In the fifth intergovernmental panel on climate change (IPCC) assessment report (IPCC, 2013; IPCC-AR5), the lower bound of the ECS estimate was revised from the fourth IPCC assessment report from 2 to 1.5 °C. In addition, the dispersion in the ECS estimate based on the energy budget and the emergent constraint (the empirical relation found in models between the ECS and observable variable) (Fasullo et al. 2015; Klein and Hall 2015) by using observation data precludes the IPCC-AR5 from providing the best estimate. These issues might be resolved at least partially by taking both ocean heat uptake and forcing efficacies into account.

Endnotes

[1]http://www.wcrp-climate.org/modelling-wgcm-mip-catalogue/modelling-wgcm-mips/418-wgcm-rfmip.

Abbreviation

AGCM, atmospheric GCM; AMOC, Atlantic meridional overturning circulation; AOGCM, atmosphere- ocean GCM; ASGCM, atmosphere-slab ocean GCM; CMIP, coupled model intercomparison project; ECS, equilibrium climate sensitivity; ERF, effective radiative forcing; GCM, general circulation model; IPCC, intergovernmental panel on climate change; IPCC-AR5, the fifth assessment report of the IPCC; UD, upwelling-diffusion; SST, sea surface temperature; TCR, transient climate response; TOA, top of the atmosphere

Acknowledgements

We thank Dr. Kyle Armour and one anonymous reviewer whose suggestions helped to greatly improve the manuscript. Dr. Armour pointed out the piecewise interpretation of Eq. (29) and drew the authors' attention to the importance of AMOC. Figure 4 was inspired by Dr. Isaac Held's blog. The authors are also thankful to the MIROC model developing team. The developers of NCL are also appreciated. Simulation data were produced by using the JAMSTEC Earth Simulator and the NIES super computer system. This work was supported by JSPS KAKENHI Grant Number 15K05280.

Authors' contributions

MY drafted the manuscript. AAO, RO, and HS provided the MIROC simulation data, and MY conducted the analysis. All of the authors made intellectual contributions to the contents and structuring of the manuscript and approved the final manuscript.

Competing interests

The authors declare that they have no competing interests.

Author details

[1]Faculty of Environmental Earth Science, Hokkaido University, Kita 10, Nishi 5, Kita-ku, Sapporo 060-0810, Japan. [2]Arctic Research Center, Hokkaido University, Sapporo, Japan. [3]Atmosphere and Ocean Research Institute, The University of Tokyo, Kashiwa, Japan. [4]Center for Global Environmental Research, National Institute for Environmental Studies, Tsukuba, Japan. [5]Japan Agency for Marine-Earth Science and Technology, Yokohama, Japan. [6]Faculty of Life and Environmental Sciences, University of Tsukuba, Tsukuba, Japan.

Received: 22 November 2015 Accepted: 12 June 2016
Published online: 18 July 2016

References

Abe Ouchi A, Saito F, Kawamura K, Raymo ME, Okuno J, Takahashi K, Blatter H (2013) Insolation-driven 100,000-year glacial cycles and hysteresis of ice-sheet volume. Nature 500:190. doi:10.1038/nature12374

Aldrin M, Holden M, Guttorp P, Skeie RB, Myhre G, Berntsen TK (2012) Bayesian estimation of climate sensitivity based on a simple climate model fitted to observations of hemispheric temperatures and global ocean heat content. Environmetrics 23:253–271. doi:10.1002/env.2140

Allen MR, Frame DJ (2007) Call off the quest. Science 318:582–583

Andrews T, Gregory JM, Forster PM, Webb MJ (2012a) Cloud adjustment and its role in CO_2 radiative forcing and climate sensitivity: a review. Surv Geophys 33:619–635

Andrews T, Gregory JM, Webb MJ (2015) The dependence of radiative forcing and feedback on evolving patterns of surface temperature change in climate models. J Clim 28:1630–1648

Andrews T, Gregory JM, Webb MJ and Taylor KE (2012b) Forcing, feedbacks and climate sensitivity in CMIP5 coupled atmosphere-ocean climate models. Geophysical Research Letters, 39:doi:Artn L09712 10.1029/2012gl051607

Andronova NG, Schlesinger ME (2001) Objective estimation of the probability density function for climate sensitivity. J Geophys Res-Atmos 106:22605–22611

Armour KC, Bitz CM, Roe GH (2013) Time-varying climate sensitivity from regional feedbacks. J Clim 26:4518–4534

Armour KC and Roe GH (2011) Climate commitment in an uncertain world. Geophysical Research Letters, 38:doi:Artn L01707 10.1029/2010gl045850

Baker MB, Roe GH (2009) The shape of things to come: why is climate change so predictable? J Clim 22:4574–4589

Bitz CM, Shell KM, Gent PR, Bailey DA, Danabasoglue G, Armour KC, Holland MM, Kiehl JT (2012) Climate sensitivity of the community climate system model, version 4. J Clim 25:3053–3070

Boe J, Hall A and Qu X (2010) Deep ocean heat uptake as a major source of spread in transient climate change simulations (vol 37, L17701, 2010). Geophysical Research Letters, 37:doi:Artn L17701 10.1029/2010gl044726

Boer GJ, Yu B (2003) Climate sensitivity and response. Clim Dyn 20:415–429

Chen XL, Zhou TJ, Guo Z (2014) Climate sensitivities of two versions of FGOALS model to idealized radiative forcing. Science China-Earth Sciences 57:1363–1373

Chung E-S, Soden BJ (2015) An assessment of methods for computing radiative forcing in climate models. Environ Res Lett 10:074004. doi:10.1088/1748-9326/10/7/074004

Collins M, Booth BBB, Harris GR, Murphy JM, Sexton DMH, Webb MJ (2006) Towards quantifying uncertainty in transient climate change. Clim Dyn 27:127–147

Colman R and McAvaney B (2009) Climate feedbacks under a very broad range of forcing. Geophysical Research Letters, 36:doi:Artn L01702 10.1029/2008gl036268

Colman RA, Power SB, McAvaney BJ (1997) Non-linear climate feedback analysis in an atmospheric general circulation model. Clim Dyn 13:717–731

Cubasch U, Meehl GA, Boer GJ, Stouffer RJ, Dix M, Noda A, Senior CA, Raper S, Yap KS (2001) Projections of future climate change. In: Houghton JT, Ding Y, Griggs DJ, Noguer M, Van Der Linden PJ, Dai X, Maskell K, Johnson CA (eds) Climate Change 2001: The Physical Science Basis. Contribution of Working Group I to the Third Assessment Report of the Intergovernmental Panel on Climate Change. Cambridge University Press, Cambridge, United Kingdom and New York, NY, USA, pp 525–582

Danabasoglu G, Gent PR (2009) Equilibrium climate sensitivity: is it accurate to use a slab ocean model? J Clim 22:2494–2499

Donohoe A, Armour KC, Pendergrass AG, Battisti DS (2014) Shortwave and longwave radiative contributions to global warming under increasing CO_2. Proc Natl Acad Sci U S A 111:16700–16705

Dufresne JL, Bony S (2008) An assessment of the primary sources of spread of global warming estimates from coupled atmosphere-ocean models. J Clim 21:5135–5144

Fasullo JT, Sanderson BM, Trenberth KE (2015) Recent progress in constraining climate sensitivity with model ensembles. Curr Climate Change Reports. doi:10.1007/s40641-015-0021-7

Feldl N, Roe GH (2013) The nonlinear and nonlocal nature of climate feedbacks. J Clim 26:8289–8304

Flato G, Marotzke J, Abiodun B, Braconnot P, Chou SC, Collins W, Cox P, Driouech F, Emori S, Eyring V, Forest C, Gleckler P, Guilyardi E, Jakob C, Kattsov V, Reason C, Rummukainen M (2013) Evaluation of climate models. In: Stocker TF, Qin D, Plattner G-K, Tignor M, Allen SK, Boschung J, Nauels A, Xia Y, Bex V, Midgley PM (eds) Climate Change 2013: The Physical Science Basis. Contribution of Working Group I to the Fifth Assessment Report of the Intergovernmental Panel on Climate Change. Cambridge University Press, Cambridge, United Kingdom and New York, NY, USA, pp 741–866

Forster PM, Andrews T, Good P, Gregory JM, Jackson LS, Zelinka M (2013) Evaluating adjusted forcing and model spread for historical and future scenarios in the CMIP5 generation of climate models. J Geophys Res-Atmos 118:1139–1150

Forster PMD, Gregory JM (2006) The climate sensitivity and its components diagnosed from Earth radiation budget data. J Clim 19:39–52

Foster G, Annan JD, Schmidt GA and Mann ME (2008) Comment on "Heat capacity, time constant, and sensitivity of Earth's climate system" by S. E. Schwartz. Journal of Geophysical Research, 113:doi:10.1029/2007jd009373

Geoffroy O, Saint-Martin D, Bellon G, Voldoire A, Olivie DJL, Tyteca S (2013a) Transient climate response in a two-layer energy-balance model. Part II: Representation of the efficacy of deep-ocean heat uptake and validation for CMIP5 AOGCMs. J Clim 26:1859–1876
Geoffroy O, Saint-Martin D, Olivie DJL, Voldoire A, Bellon G, Tyteca S (2013b) Transient climate response in a two-layer energy-balance model. Part I: analytical solution and parameter calibration using CMIP5 AOGCM experiments. J Clim 26:1841–1857
Geoffroy O, Saint-Martin D and Ribes A (2012) Quantifying the sources of spread in climate change experiments. Geophysical Research Letters, 39:doi:Artn L24703 10.1029/2012gl054172
Gregory J, Webb M (2008) Tropospheric adjustment induces a cloud component in CO_2 forcing. J Clim 21:58–71
Gregory JM (2000) Vertical heat transports in the ocean and their effect an time-dependent climate change. Clim Dyn 16:501–515
Gregory JM, Andrews T, Good P (2015) The inconsistency of the transient climate response parameter under increasing CO_2. Phil Trans R Soc A 373:20140417
Gregory JM and Forster PM (2008) Transient climate response estimated from radiative forcing and observed temperature change. Journal of Geophysical Research-Atmospheres, 113:doi:Artn D23105 10.1029/2008jd010405
Gregory JM, Ingram WJ, Palmer MA, Jones GS, Stott PA, Thorpe RB, Lowe JA, Johns TC and Williams KD (2004) A new method for diagnosing radiative forcing and climate sensitivity. Geophysical Research Letters, 31:doi:Artn L03205 10.1029/2003gl018747
Gregory JM, Jones CD, Cadule P, Friedlingstein P (2009) Quantifying carbon cycle feedbacks. J Clim 22:5232–5250
Gregory JM, Jones CD, Cadule P, Friedlingstein P (2010) Quantifying carbon cycle feedbacks (vol 22, pg 5232, 2009). J Clim 23:6706–6707
Gregory JM, Mitchell JFB (1997) The climate response to CO_2 of the Hadley Centre coupled AOGCM with and without flux adjustment. Geophys Res Lett 24:1943–1946
Gregory JM, Stouffer RJ, Raper SCB, Stott PA, Rayner NA (2002) An observationally based estimate of the climate sensitivity. J Clim 15:3117–3121
Hansen J, Johnson D, Lacis A, Lebedeff S, Lee P, Rind D, Russell G (1981) Climate impact of increasing atmospheric carbon dioxide. Science 213:957–966
Hansen J, Lacis A, Rind D, Russell G, Stone P, Fung I, Ruedy R and Lerner J (1984) Climate sensitivity: analysis of feedback mechanisms. Hansen, J.E. and T. Takahashi (eds.): Climate Processes and Climate Sensitivity, Geophysical Monograph Series, 29, AGU, Washington, D. C., USA, 130-163.
Hansen J, Russell G, Lacis A, Fung I, Rind D, Stone P (1985) Climate response times: dependence on climate sensitivity and ocean mixing. Science 229:857–859
Hansen J, Sato M, Ruedy R (1997) Radiative forcing and climate response. J Geophys Res-Atmos 102:6831–6864
Hansen J, Sato M, Ruedy R, Nazarenko L, Lacis A, Schmidt GA, Russell G, Aleinov I, Bauer M, Bauer S, Bell N, Cairns B, Canuto V, Chandler M, Cheng Y, Del Genio A, Faluvegi G, Fleming E, Friend A, Hall T, Jackman C, Kelley M, Kiang N, Koch D, Lean J, Lerner J, Lo K, Menon S, Miller R, Minnis P, Novakov T, Oinas V, Perlwitz J, Perlwitz J, Rind D, Romanou A, Shindell D, Stone P, Sun S, Tausnev N, Thresher D, Wielicki B, Wong T, Yao M and Zhang S (2005) Efficacy of climate forcings. Journal of Geophysical Research-Atmospheres, 110:doi:Artn D18104 10.1029/2005jd005776
Held IM, Winton M, Takahashi K, Delworth T, Zeng FR, Vallis GK (2010) Probing the fast and slow components of global warming by returning abruptly to preindustrial forcing. J Clim 23:2418–2427
IPCC (2013) Climate change 2013: the physical science basis. In: Stocker TF, Qin D, Plattner G-K, Tignor M, Allen SK, Boschung J, Nauels A, Xia Y, Bex V, Midgley PM (eds) Contribution of Working Group I to the Fifth Assessment Report of the Intergovernmental Panel on Climate Change. Cambridge University Press, Cambridge, United Kingdom and New York, NY, USA, p 1535
Ishizaki Y, Shiogama H, Emori S, Yokohata T, Nozawa T, Ogura T, Abe M, Yoshimori M, Takahashi K (2012) Temperature scaling pattern dependence on representative concentration pathway emission scenarios. Clim Chang 112:535–546
Ishizaki Y, Shiogama H, Emori S, Yokohata T, Nozawa T, Takahashi K, Ogura T, Yoshimori M, Nagashima T (2013) Dependence of precipitation scaling patterns on emission scenarios for representative concentration pathways. J Clim 26:8868–8879
Johansson DJA, O'Neill BC, Tebaldi C, Häggström O (2015) Equilibrium climate sensitivity in light of observations over the warming hiatus. Nat Clim Chang 5:449–453
Jonko AK, Shell KM, Sanderson BM, Danabasoglu G (2013) Climate feedbacks in CCSM3 under changing CO_2 forcing. Part II: variation of climate feedbacks and sensitivity with forcing. J Climate 26:2784–2795
K-1 model developers (2004) K-1 coupled GCM (MIROC) description. Tech. rep., Center for Climate System Research, The University of Tokyo, Tokyo, Japan.
Kamae Y, Watanabe M, Ogura T, Yoshimori M, Shiogama H (2015) Rapid adjustments of cloud and hydrological cycle to increasing CO2: a review. Curr Clim Change Rep 1:103–113
Kiehl JT, Shields CA, Hack JJ, Collins WD (2006) The climate sensitivity of the community climate system model version 3 (CCSM3). J Clim 19:2584–2596
Klein SA, Hall A (2015) Emergent constraints for cloud feedbacks. Curr Clim Change Rep. doi:10.1007/s40641-015-0027-1
Knutti R, Hegerl GC (2008) The equilibrium sensitivity of the Earth's temperature to radiation changes. Nat Geosci 1:735–743
Knutti R, Krähenmann S, Frame DJ and Allen MR (2008) Comment on "Heat capacity, time constant, and sensitivity of Earth's climate system" by S. E. Schwartz. Journal of Geophysical Research, 113:doi:10.1029/2007jd009473
Knutti R, Stocker TF (2000) Influence of the thermohaline circulation on projected sea level rise. J Clim 13:1997–2001
Kosaka Y, Xie SP (2013) Recent global-warming hiatus tied to equatorial Pacific surface cooling. Nature 501:403–407
Kostov Y, Armour KC, Marshall J (2014) Impact of the Atlantic meridional overturning circulation on ocean heat storage and transient climate change. Geophys Res Lett 41:2108–2116
Kuhlbrodt T and Gregory JM (2012) Ocean heat uptake and its consequences for the magnitude of sea level rise and climate change. Geophysical Research Letters, 39:doi:Artn L18608, 10.1029/2012gl052952
Kummer JR, Dessler AE (2014) The impact of forcing efficacy on the equilibrium climate sensitivity. Geophys Res Lett 41:3565–3568. doi:10.1002/2014gl060046
Lewis N, Curry JA (2015) The implications for climate sensitivity of AR5 forcing and heat uptake estimates. Clim Dyn 45:1009–1023
Li C, von Storch JS, Marotzke J (2013) Deep-ocean heat uptake and equilibrium climate response. Clim Dyn 40:1071–1086
Long DJ, Collins M (2013) Quantifying global climate feedbacks, responses and forcing under abrupt and gradual CO_2 forcing. Clim Dyn 41:2471–2479
Marshall DP, Zanna L (2014) A conceptual model of ocean heat uptake under climate change. J Clim 27:8444–8465
Marvel K, Schmidt GA, Miller RK, Nazarenko LS (2015) Implications for climate sensitivity from the response to individual forcings. Nat Clim Chang. doi:10.1038/NCLIMATE2888
Maslin M, Austin P (2012) Climate models at their limit? Nature 486:183–184
Masters T (2014) Observational estimate of climate sensitivity from changes in the rate of ocean heat uptake and comparison to CMIP5 models. Clim Dyn 42:2173–2181
Meehl GA, Arblaster JM, Fasullo JT, Hu AX, Trenberth KE (2011) Model-based evidence of deep-ocean heat uptake during surface-temperature hiatus periods. Nat Clim Chang 1:360–364
Meehl GA, Washington WM, Collins WD, Arblaster JM, Hu A, Buja LE, Strand WG, Teng H (2005) How much more global warming and sea level rise? Science 307:1769–1772
Meraner K, Mauritsen T, Voigt A (2013) Robust increase in equilibrium climate sensitivity under global warming. Geophys Res Lett 40:5944–5948
Merlis TM, Held IM, Stenchikov GL, Zeng FR, Horowitz LW (2014) Constraining transient climate sensitivity using coupled climate model simulations of volcanic eruptions. J Clim 27:7781–7795
Murphy JM (1995) Transient-response of the Hadley Center coupled ocean-atmosphere model to increasing carbon-dioxide.3. Analysis of global-mean response using simple-models. J Clim 8:496–514
Otto A, Otto FEL, Boucher O, Church J, Hegerl G, Forster PM, Gillett NP, Gregory J, Johnson GC, Knutti R, Lewis N, Lohmann U, Marotzke J, Myhre G, Shindell D, Stevens B, Allen MR (2013) Energy budget constraints on climate response. Nat Geosci 6:415–416
Plattner GK, Knutti R, Joos F, Stocker TF, von Bloh W, Brovkin V, Cameron D, Driesschaert E, Dutkiewicz S, Eby M, Edwards NR, Fichefet T, Hargreaves JC, Jones CD, Loutre MF, Matthews HD, Mouchet A, Muller SA, Nawrath S, Price A, Sokolov A, Strassmann KM, Weaver AJ (2008) Long-term climate commitments projected with climate-carbon cycle models. J Clim 21:2721–2751
Raper SCB, Gregory JM, Stouffer RJ (2002) The role of climate sensitivity and ocean heat uptake on AOGCM transient temperature response. J Clim 15:124–130

Rhein M, Rintoul SR, Aoki S, Campos E, Chambers D, Feely RA, Gulev S, Johnson GC, Josey SA, Kostianoy A, Mauritzen C, Roemmich D, Talley LD, Wang F (2013) Observations: ocean. In: Stocker TF, Qin D, Plattner G-K, Tignor M, Allen SK, Boschung J, Nauels A, Xia Y, Bex V, Midgley PM (eds) Climate Change 2013: The Physical Science Basis. Contribution of Working Group I to the Fifth Assessment Report of the Intergovernmental Panel on Climate Change. Cambridge University Press, Cambridge, United Kingdom and New York, NY, USA, pp 255–315
Rose BEJ, Armour KC, Battisti DS, Feldl N, Koll DDB (2014) The dependence of transient climate sensitivity and radiative feedbacks on the spatial pattern of ocean heat uptake. Geophys Res Lett 41:1071–1078
Scafetta N (2009) Empirical analysis of the solar contribution to global mean air surface temperature change. J Atmospheric Solar-Terrestrial Physics 71:1916–1923
Schwartz SE (2007) Heat capacity, time constant, and sensitivity of Earth's climate system. Journal of Geophysical Research-Atmospheres, 112:doi:Artn D24s05 10.1029/2007jd008746
Schwartz SE (2008) Reply to comments by G. Foster et al., R. Knutti et al., and N. Scafetta on "Heat capacity, time constant, and sensitivity of Earth's climate system". Journal of Geophysical Research, 113:doi:10.1029/2008jd009872
Senior CA, Mitchell JFB (2000) The time-dependence of climate sensitivity. Geophys Res Lett 27:2685–2688
Shell KM (2013) Consistent differences in climate feedbacks between atmosphere-ocean GCMs and atmospheric GCMs with slab-ocean models. J Clim 26:4264–4281
Sherwood SC, Bony S, Boucher O, Bretherton C, Forster PM, Gregory JM, Stevens B (2015) Adjustments in the forcing-feedback framework for understanding climate change. Bull Am Meteorol Soc 96:217–228
Shindell DT (2014) Inhomogeneous forcing and transient climate sensitivity. Nat Clim Chang 4:274–277
Shindell DT, Faluvegi G, Rotstayn L, Milly G (2015) Spatial patterns of radiative forcing and surface temperature response. J Geophys Res-Atmos 120:5385–5403
Shine KP, Cook J, Highwood EJ and Joshi MM (2003) An alternative to radiative forcing for estimating the relative importance of climate change mechanisms. Geophysical Research Letters, 30:doi:Artn 2047 10.1029/2003gl018141
Siegenthaler U, Oeschger H (1984) Transient temperature-changes due to increasing CO_2 using simple-models. Ann Glaciol 5:153–159
Skeie RB, Berntsen T, Aldrin M, Holden M, Myhre G (2014) A lower and more constrained estimate of climate sensitivity using updated observations and detailed radiative forcing time series. Earth System Dynamics 5:139–175
Solomon S, Plattner GK, Knutti R, Friedlingstein P (2009) Irreversible climate change due to carbon dioxide emissions. Proc Natl Acad Sci U S A 106:1704–1709
Stouffer RJ, Manabe S (1999) Response of a coupled ocean-atmosphere model to increasing atmospheric carbon dioxide: sensitivity to the rate of increase. J Clim 12:2224–2237
Stuber N, Sausen R, Ponater M (2001) Stratosphere adjusted radiative forcing calculations in a comprehensive climate model. Theor Appl Climatol 68:125–135
Taylor KE, Stouffer RJ, Meehl GA (2012) An overview of CMIP5 and the experiment design. Bull Am Meteorol Soc 93:485–498
Watanabe M, Kamae Y, Yoshimori M, Oka A, Sato M, Ishii M, Mochizuki T, Kimoto M (2013) Strengthening of ocean heat uptake efficiency associated with the recent climate hiatus. Geophys Res Lett 40:3175–3179
Watanabe M, Shiogama H, Tatebe H, Hayashi M, Ishii M, Kimoto M (2014) Contribution of natural decadal variability to global warming acceleration and hiatus. Nat Clim Chang 4:893–897
Watterson IG (2000) Interpretation of simulated global warming using a simple model. J Clim 13:202–215
Wigley TM, Raper SC (2001) Interpretation of high projections for global-mean warming. Science 293:451–454
Wigley TML, Schlesinger ME (1985) Analytical solution for the effect of increasing CO_2 on global mean temperature. Nature 315:649–652
Williams KD, Ingram WJ, Gregory JM (2008) Time variation of effective climate sensitivity in GCMs. J Clim 21:5076–5090
Winton M, Adcroft A, Griffies SM, Hallberg RW, Horowitz LW, Stouffer RJ (2013a) Influence of ocean and atmosphere components on simulated climate sensitivities. J Clim 26:231–245
Winton M, Griffies SM, Samuels BL, Sarmiento JL, Frolicher TL (2013b) Connecting changing ocean circulation with changing climate. J Clim 26:2268–2278
Winton M, Takahashi K, Held IM (2010) Importance of ocean heat uptake efficacy to transient climate change. J Clim 23:2333–2344
Yamamoto A, Abe-Ouchi A, Shigemitsu M, Oka A, Takahashi K, Ohgaito R, Yamanaka Y (2015) Global deep ocean oxygenation by enhanced ventilation in the Southern Ocean under long-term global warming. Glob Biogeochem Cycles 29:1801–1815
Yamamoto A, Yamanaka Y, Oka A, Abe-Ouchi A (2014) Ocean oxygen depletion due to decomposition of submarine methane hydrate. Geophys Res Lett 41: 5075–5083
Yokohata T, Emori S, Nozawa T, Ogura T, Kawamiya M, Tsushima Y, Suzuki T, Yukimoto S, Abe-Ouchi A, Hasumi H, Sumi A, Kimoto M (2008) Comparison of equilibrium and transient responses to CO_2 increase in eight state-of-the-art climate models. Tellus Series a-Dynamic Meteorol Oceanography 60:946–961
Yoshimori M, Abe-Ouchi A (2012) Sources of spread in multimodel projections of the Greenland Ice Sheet surface mass balance. J Clim 25:1157–1175
Yoshimori M, Broccoli AJ (2008) Equilibrium response of an atmosphere-mixed layer ocean model to different radiative forcing agents: global and zonal mean response. J Clim 21:4399–4423
Yoshimori M, Hargreaves JC, Annan JD, Yokohata T, Abe-Ouchi A (2011) Dependency of feedbacks on forcing and climate state in physics parameter ensembles. J Clim 24:6440–6455
Yoshimori M, Yokohata T, Abe-Ouchi A (2009) A comparison of climate feedback strength between CO_2 doubling and LGM experiments. J Clim 22:3374–3395
Yoshimori M, Watanabe M, Abe-Ouchi A, Shiogama H, Ogura T (2014) Relative contribution of feedback processes to Arctic amplification of temperature change in MIROC GCM. Clim Dyn 42:1613–1630
Zickfeld K, Eby M, Weaver AJ, Alexander K, Crespin E, Edwards NR, Eliseev AV, Feulner G, Fichefet T, Forest CE, Friedlingstein P, Goosse H, Holden PB, Joos F, Kawamiya M, Kicklighter D, Kienert H, Matsumoto K, Mokhov II, Monier E, Olsen SM, Pedersen JOP, Perrette M, Philippon-Berthier G, Ridgwell A, Schlosser A, Von Deimling TS, Shaffer G, Sokolov A, Spahni R, Steinacher M, Tachiiri K, Tokos KS, Yoshimori M, Zeng N, Zhao F (2013) Long-term climate change commitment and reversibility: an EMIC intercomparison. J Clim 26:5782–5809